Supplementary Item 4. Quantifying diffusional fluxes of REEs into melt inclusions

Spandler et al. (2007) re-equilibrated natural olivine phenocrysts separated from a mid-ocean ridge basalt in a synthetic basalt doped with five of the REEs – Pr, Eu, Tb, Ho and Lu. The olivine phenocrysts hosted melt inclusions, as many such olivine phenocrysts do. These experiments record diffusion of the REEs in two different, independent ways. Firstly, analysis of the olivine revealed conventional diffusion profiles from the olivine-phenocryst/synthetic-basalt interfaces, from which diffusion coefficients were calculated in the usual way from concentration as a function of distance. Secondly, the fluxes of the REEs through the olivine phenocrysts were recorded by analysing the increase in REEs in the melt inclusions. These experiments were, to our knowledge, the first to measure the fluxes of trace elements through any mineral independently of concentration/distance profiles. The distinction is important, because the fluxes so measured provide evidence that the pathway of diffusion was through the crystal lattice rather than along extended defects (unlikely though it may be that any extended defects would provide pathways covering the 10^2 μm scale of the concentration/distance profiles in these experiments anyway).

Examples of the changes in REE content of the melt inclusions were shown in Fig. 1 of Spandler et al. (2007). The increases in the doped REEs in the melt inclusions were up to three orders of magnitude larger than their original REE concentrations. The increased concentrations of the five doped REEs in any given inclusion show a smooth correlation with the REE olivine/melt partition coefficients, which is shown in Fig. A4.1 for the four most re-equilibrated inclusions from the 25-day experiment, by plotting their normalized concentrations, c^*_{REE}, against the olivine/melt partition coefficient, K_{REE}. The normalized concentration is $(c^{REE}_{obs} - c^{REE}_{o}) / (c^{REE}_{o} - c^{REE}_{ex})$, where c^{REE}_{obs} is the observed concentration in the melt inclusion, c^{REE}_{o} is the presumed initial concentration, taken as the mean concentration of the inclusions hosted in olivines not used in the experiments, and c^{REE}_{ex} is the concentration in the external melt.

While Fig. A4.1 establishes that the values of c^*_{REE} vary smoothly with K_{REE} for a given inclusion, we can go further and show that the magnitude of this variation is that expected from the variation in K_{REE} among the five REE doped in the experiments. The mathematic model of Qin et al. (1992) describing the diffusive re-equilibration of a melt inclusion treats a spherical melt inclusion hosted at the centre of a spherical crystal immersed in a melt of different composition to the inclusion. The modelling includes an equation describing the change in concentration of a species M in the melt inclusion with time, $c^M(t)$. Their solution (their Eqn. 10) is not fully analytic, in that it includes the summation of an infinite series of roots to a transcendental equation, which must be obtained numerically. For our purposes, therefore, some simplification is required. The essential features of Eqn. 10 of Qin et al. may be summarized as:

$$c^M_{obs} = c^M_o + K_M(c^M_o - c^M_{ex}) \,.\, f(a, b, D_M, K_M) \qquad \text{(A4.2)}$$

where a is the radius of the melt inclusion, b the radius of the crystal, D_M the diffusion coefficient and K_M the crystal/melt partition coefficient. The idealized geometry assumed by Qin et al. is rather an approximate description of reality, but conceptually the function $f(a, b, D_M, K_M)$ could be expanded to include a geometrical factor ϕ to account for real situations with non-spherical

inclusions positioned off centre of non-spherical crystals. For simplicity we write this function for each element in each inclusion as f_M. Eqn. 4.2 is conveniently rearranged to:

$$\frac{(c^M_{obs} - c^M_o)}{(c^M_o - c^M_{ex})} = c^*_M = K_M \cdot f_M \qquad \text{(A4.2a)}$$

One of the findings of Spandler et al. (2007) was that the diffusion coefficients of all the REEs were the same. Then f_{REE} should be the same for each REE in each melt inclusion, except for its dependence on K_{REE}. We assume that the dependence on K_{REE} is of second-order importance, and designate one of the REE as a reference; the obvious candidate is Tb, because it is the mid REE in atomic number of the five REE studied by Spandler et al. (2007). We would then expect that:

$$c^*_{REE} \approx c^*_{Tb} \frac{K_{REE}}{K_{Tb}} \qquad \text{(A4.3)}$$

If c^*_{REE} for the REE other than Tb are plotted against c^*_{Tb}, they should fall on straight lines passing through the origin, as shown in Fig. A4.2, with a slope of K_{REE}/K_{Tb}. The values of the slopes are compared to K_{REE}/K_{Tb} measured directly, from the concentrations at the olivine/melt interfaces, in Fig. A4.3. It may be added that these direct measurements of K_{REE}/K_{Tb} are in excellent agreement with values from recent equilibrium partitioning experiments (Evans et al. 2008). This evaluation demonstrates that the diffusion mechanism for the REEs in the Spandler et al. experiments was unambiguously lattice diffusion.

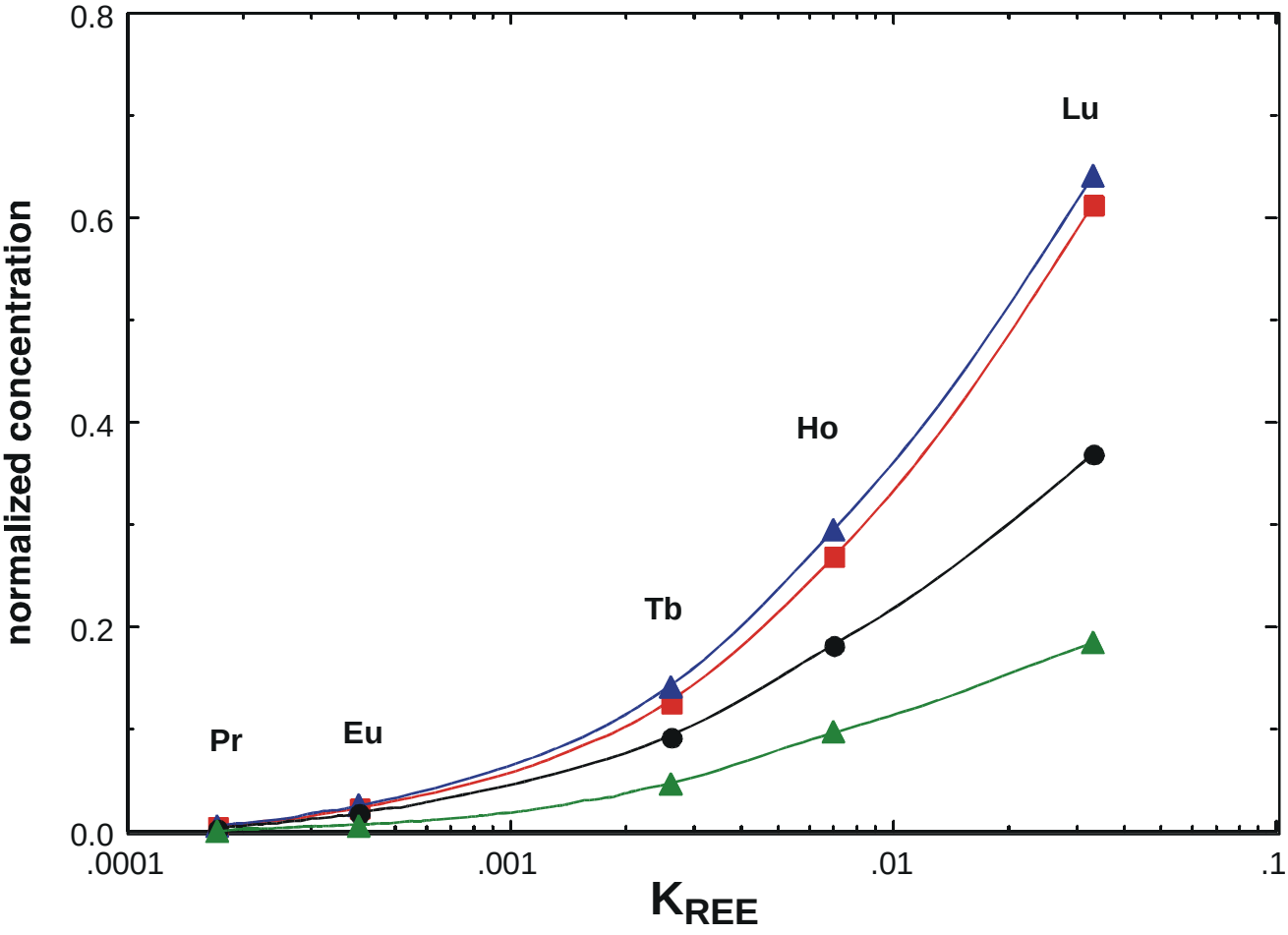

Fig. A4.1 Normalized concentrations of REEs in the four most equilibrated melt inclusions from the 25-day experiment of Spandler et al. (2007), plotted against the olivine/melt partition coefficient calculated from the mean values of c_o (the concentration in olivine the olivine/melt interface) refined from fitting the diffusion profiles. Note the smooth trends.

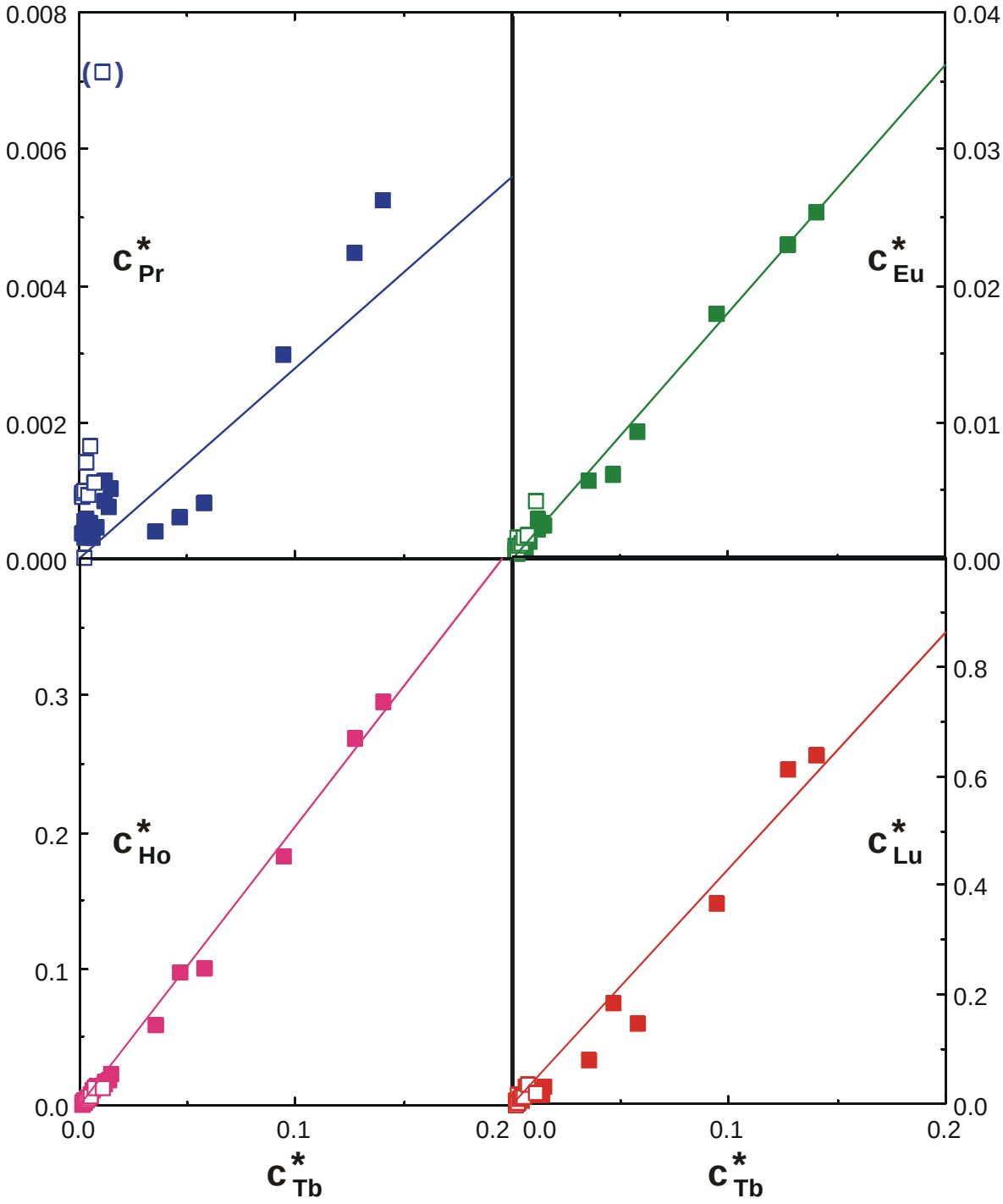

Fig. A4.2. Values of c^*_{REE} for Pr, Eu, Ho and Lu plotted against c^*_{Tb} from the 25-day (solid symbols) and 5-day (open symbols) experiments of Spandler et al. (2007). The arrays form straight lines that pass through the origin. The values of c^*_{Pr} show considerable scatter at low degrees of re-equilibration because the variability in the initial concentrations of the melt inclusions is significant compared to the extent of re-equilibration.

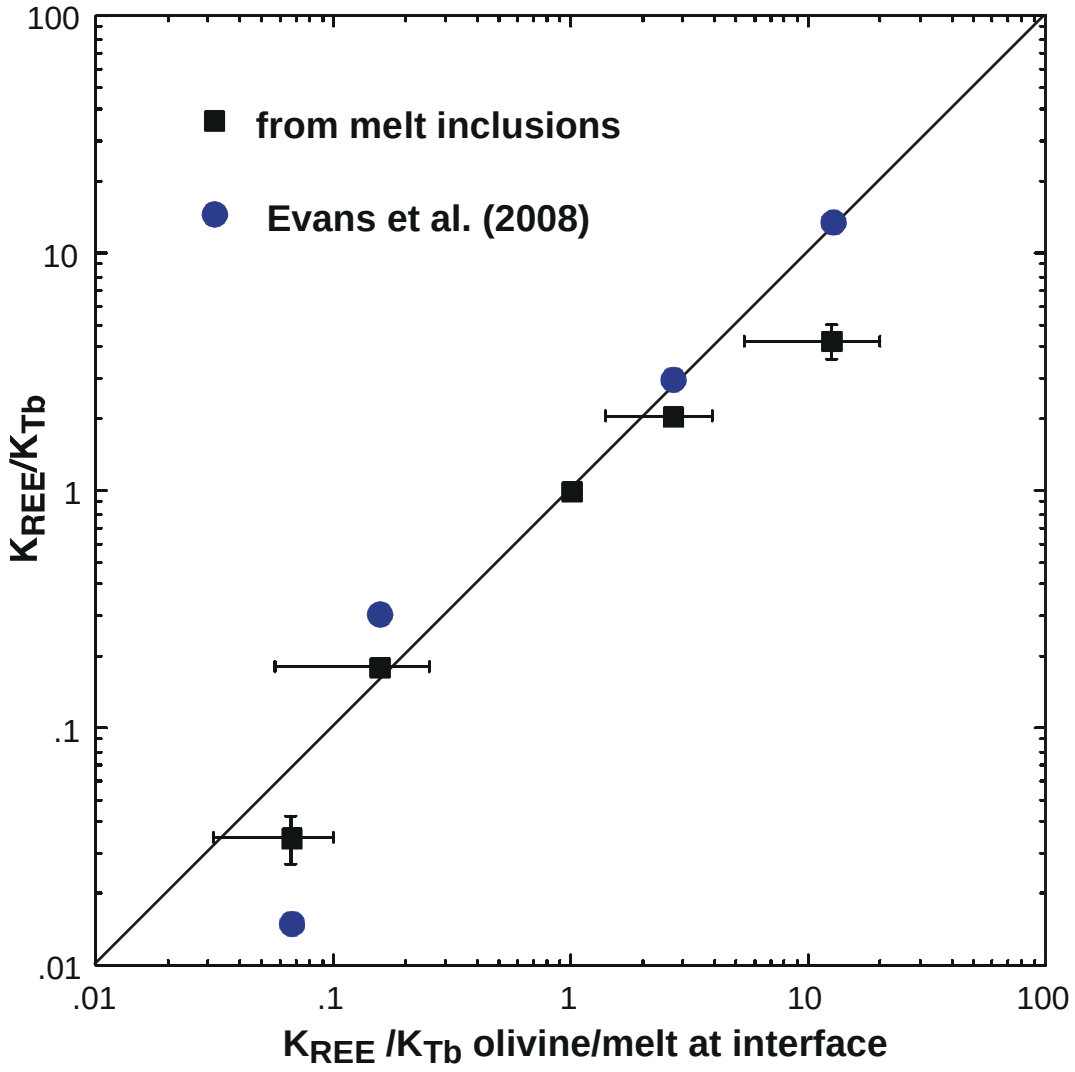

Fig. A4.3. The slopes of the arrays in Fig. A4.2, which should be approximately K_{REE}/K_{Tb} (Eqn. A4.3) plotted against the values of K_{REE}/K_{Tb} obtained directly by Spandler et al. (2007). Also shown are the mean values of K_{REE}/K_{Tb} from olivine/melt equilibrium partitioning experiments on 10 melt compositions in the system CaO-MgO-Al_2O_3-SiO_2 at 1400 ºC from Evans et al. (2008).